To what extent does the Eddy Covariance footprint cutoff influence the estimation of surface energy fluxes using two source energy balance model and high-resolution imagery in commercial vineyards?

Nassar, Ayman, Torres-Rua, Alfonso, Kustas, William, Nieto, Hector, McKee, Mac, et al.

Ayman Nassar, Alfonso Torres-Rua, William Kustas, Hector Nieto, Mac McKee, Lawrence Hipps, Joseph Alfieri, John Prueger, Maria Mar Alsina, Lynn McKee, Calvin Coopmans, Luis Sanchez, Nick Dokoozlian, "To what extent does the Eddy Covariance footprint cutoff influence the estimation of surface energy fluxes using two source energy balance model and high-resolution imagery in commercial vineyards?," Proc. SPIE 11414, Autonomous Air and Ground Sensing Systems for Agricultural Optimization and Phenotyping V, 114140G (26 May 2020); doi: 10.1117/12.2558777

SPIE.

Event: SPIE Defense + Commercial Sensing, 2020, Online Only

To What Extend Does the Eddy Covariance Footprint Cutoff Influence the Estimation of Surface Energy Fluxes Using Two Source Energy Balance Model and High-Resolution Imagery in Commercial Vineyards?

Ayman Nassar [a,*], Alfonso Torres-Rua [a], William Kustas [b], Hector Nieto [c], Mac McKee [a], Lawrence Hipps [d], Joseph Alfieri [b], John Prueger [e], Maria Mar Alsina [f], Lynn McKee [b], Calvin Coopmans [g], Luis Sanchez [f] and Nick Dokoozlian [f]

[a] Department of Civil and Environmental Engineering, Utah State University, Logan, UT 84322, USA; Alfonso.Torres@usu.edu (A.F.T.-R.); mac.mckee@usu.edu (M.M.)

[b] U. S. Department of Agriculture, Agricultural Research Service, Hydrology and Remote Sensing Laboratory, Beltsville, MD 20705, USA; bill.kustas@usda.gov (W.P.K.); Joe.Alfieri@ars.usda.gov (J.A); lynn.mckee@ars.usda.gov (L.M.)

[c] Complutum Tecnologías de la Información Geográfica (COMPLUTIG), Madrid, Spain; hector.nieto@complutig.com (H.N.)

[d] Plants, Soils and Climate Department, Utah State University, Logan, UT 84322, USA; Lawrence.Hipps@usu.edu (L.H.)

[e] U. S. Department of Agriculture, Agricultural Research Service, National Laboratory for Agriculture and the Environment, Ames, IA 50011, USA; john.prueger@usda.gov (J.H.P.)

[f] E & J Gallo Winery Viticulture Research, Modesto, CA 95354, USA; MariadelMar.Alsina@ejgallo.com (M.M.A.);

Luis.Sanchez@ejgallo.com (L.S.); Nick.Dokoozlian@ejgallo.com (N.D.)

[g] Department of Electrical Engineering, Utah State University, Logan, UT 84322, USA; cal.coopmans@usu.edu

(C.C.)

* Correspondence: aymnassar@aggiemail.usu.edu

ABSTRACT

Validation of surface energy fluxes from remote sensing sources is performed using instantaneous field measurements obtained from eddy covariance (EC) instrumentation. An eddy covariance measurement is characterized by a footprint function / weighted area function that describes the mathematical relationship between the spatial distribution of surface flux sources and their corresponding magnitude. The orientation and size of each flux footprint / source area depends on the micro-meteorological conditions at the site as measured by the EC towers, including turbulence fluxes, friction velocity (u_{star}), and wind speed, all of which influence the dimensions and orientation of the footprint. The total statistical weight of the footprint is equal to unity. However, due to the large size of the source area / footprint, a statistical weight cutoff of less than one is considered, ranging between 0.85 and 0.95, to ensure that the footprint model is located inside the study area. This results in a degree of uncertainty when comparing the modeled fluxes from remote sensing energy models (i.e., TSEB2T) against the EC field measurements. In this research effort, the sensitivity of instantaneous and daily surface energy flux estimates to footprint weight cutoffs are evaluated using energy balance fluxes estimated with multispectral imagery acquired by AggieAir sUAS (small Unmanned Aerial

Autonomous Air and Ground Sensing Systems for Agricultural Optimization and Phenotyping V, edited by J. Alex Thomasson, Alfonso F. Torres-Rua, Proc. of SPIE Vol. 11414, 114140G
 · doi: 10.1117/12.2558777

Vehicle) over commercial vineyards near Lodi, California, as part of the ARS-USDA Agricultural Research Service's Grape Remote Sensing Atmospheric Profile and Evapotranspiration eXperiment (GRAPEX) project. The instantaneous fluxes from the eddy covariance tower will be compared against instantaneous fluxes obtained from different TSEB2T aggregated footprint weights (cutoffs). The results indicate that the size, shape, and weight of pixels inside the footprint source area are strongly influenced by the cutoff values. Small cutoff values, such as 0.3 and 0.35, yielded high weights for pixels located within the footprint domain, while large cutoffs, such as 0.9 and 0.95, result in low weights. The results also indicate that the distribution of modelled LE values within the footprint source area are influenced by the cutoff values. A wide variation in LE was observed at high cutoffs, such as 0.90 and 0.95, while a low variation was observed at small cutoff values, such as 0.3. This happens due to the large number of pixel units involved inside the footprint domain when using high cutoff values, whereas a limited number of pixels are obtained at lower cutoff values.

Keywords: eddy covariance (EC), footprint / source area, energy fluxes, latent heat flux (LE), spatial analysis, footprint cutoff, TSEB2T model, Kljun EC footprint model.

1. INTRODUCTION

Quantifying surface energy fluxes is essential for studying land-atmosphere interactions to better understand the physics behind climate and weather. Several methods have been used to measure surface fluxes in the field; however, the eddy covariance (EC) system has gained more popularity because it has few theoretical assumptions and an extensive scope of applications. For that reason, micrometeorologists consider it a standard method for determining energy and substance fluxes [1]. Even so, the spatial heterogeneity of the land surface could be a challenging issue for EC measurements and limits its use. However, several studies have found the EC system capable of accurately measuring fluxes in a forest when the fluxes above and below canopy were partitioned [2,3,4,5]. The EC tower is described as a non-intrusive technique that can spatially integrate fluxes at the ecosystem scale with a spatial domain of a few hectares [6]. This contrasts with the flux chamber, which focuses on homogenous areas with a spatial domain not to exceed $1m^2$ [7].

The presence of different vegetation types and land cover patches at field scale may entail issues related to the representative spatial domain of the EC measurements [6]. This stems from the fact that the EC integration process for measuring fluxes is non-uniform and potentially results in different contributions from different land cover types [8]. The relative spatial weight of EC is defined as the footprint / source area, which depends on the micro-meteorological conditions at the site as measured by the EC tower. These conditions include turbulence fluxes, friction velocity (u_{star}), and wind speed, all of which influence the dimensions (fetch) and orientation of the footprint. The footprint dimension is determined by the EC fetch analysis that identifies the maximum distance between the EC tower and the extent of the source area. The total statistical weight of the footprint is equal to unity. For large source areas (~100%) the EC footprint has the potential to exceed the study area in an unacceptable way.

Applying the footprint models has become a standard task for flux tower measurement analysis [9,10], and these footprint models are essential for validating the results of surface energy flux models such as the Two-Source Energy Balance Model (TSEB) and others. Although widespread footprint models have been used in different applications, the selection of suitable models still presents some challenges [11], and it is still in the exploratory stage. Another prominent challenge to the use of footprint models is related to the footprint weight cutoff, which could vary up to ~1. Few previous studies have addressed the suitable footprint weight cutoff, particularly in heterogeneous areas. Anderson and Vivoni 2016 [12] pointed out that cutoff values between 30% and 80% had low sensitivity when using the Kormann and Meixner model to measure land surface fluxes over a vegetation area. Still, the process of determining the cutoff value of an EC footprint source area is in the exploratory stage, particularly in complex canopy environments such as vineyards. In this research effort, multiple EC cutoff values have been tested to determine how the surface energy fluxes are influenced by the spatial extension of the footprint. The Kljun et al. 2015 [11] model was used at multiple cutoff values (0.3, 0.35, 0.4, 0.45, 0.5, 0.55, 0.6, 0.65, 0.7, 0.75, 0.8, 0.85, 0.9, and 0.95), along with the TSEB2T model, to calculate the surface energy fluxes, mainly the latent heat flux (LE).

2. METHODOLOGY

2.1 Study area

The experiment was carried out in a vineyard with an area of approximately 62 ha located near Lodi in California's Central Valley (38.29 N, 121.12 W) [13,14]. The vineyard is operated and managed by Pacific Agri-Lands Management in cooperation with E&J Gallo Winery. The plantation structure is oriented east-west with a row width of 3.35 m (11 feet). A cover crop grows in the interrows at a width of ~2-m, with bare soil strips along the vine rows, spanning ~ 0.7 m. The vine height varies between 2 m and 2.5 m agl (above ground level), and the plant biomass is concentrated in the upper half of the canopy height. The study site has been a part of the Grape Remote sensing Atmospheric Profile and Evapotranspiration eXperiment (GRAPeX) program for several years. This program is conducted as a collaboration between the USDA Agricultural Research Service, E&J Gallo Winery, Utah State University, University of California in Davis, and others [15,16].

Flight campaigns were carried out by the AggieAir sUAS Program at Utah State University (https://uwrl.usu.edu/aggieair/). Multispectral images of the entire field have been acquired through many sUAS campaigns over several growing seasons. Optical data involving red, green, blue, and near infrared bands were acquired at 10-cm spatial resolution [17,18,19]. Land surface temperature (LST) was acquired during the same flights using a microbolometer camera [20] and was radiometrically calibrated [21] using the procedures discussed in Torres-Rua 2017 [22].

To evaluate the ET performance, an eddy covariance (EC) flux system was deployed to measure turbulent fluxes, including LE and H, and the available energy terms of R_n and G. The tower is located at the eastern edge of the field due to predominant winds from the west. EC micrometeorological data also included wind speed, air temperature, vapor pressure, air pressure, and shortwave radiation. Hourly average values of these atmospheric forcing variables, as well as the components of the surface energy balance, were computed. Table (1) illustrates the in-situ micrometeorological parameters and the names of the instruments used for the measurements.

Table 1. Description of in-situ micrometeorological measurements in this study.

ID	Micrometeorological parameters	Instrument name[1]	Elevation
1	Water vapor concentration	Infrared gas analyzer (EC150, Campbell Scientific, Logan, Utah)	5 m agl
2	Wind velocity	Sonic anemometer (CSAT3, Campbell Scientific)	5 m agl
3	Net radiation	4-way radiometer (CNR-1, Kipp and Zonen, Delft, Netherlands)	6 m agl
4	Air temperature	Gill shielded temperature (Vaisala, Helsinki, Finland)	5 m agl
5	Water vapor pressure	Humidity probe (HMP45C, Vaisala, Helsinki, Finland)	5 m agl
6	Soil heat flux	Five plates (HFT-3, Radiation Energy Balance Systems, Bellevue, Washington)	-8 cm
7	Soil temperature	Thermocouples	-2 cm
8	Soil moisture	Soil moisture probe (HydraProbe, Stevens Water Monitoring Systems, Portland, Oregon)	-5 cm

[1] The use of trade, firm, or corporation names in this article is for the information and convenience of the reader. Such use does not constitute official endorsement or approval by the US Department of Agriculture or the Agricultural Research Service of any product or service to the exclusion of others that may be suitable.

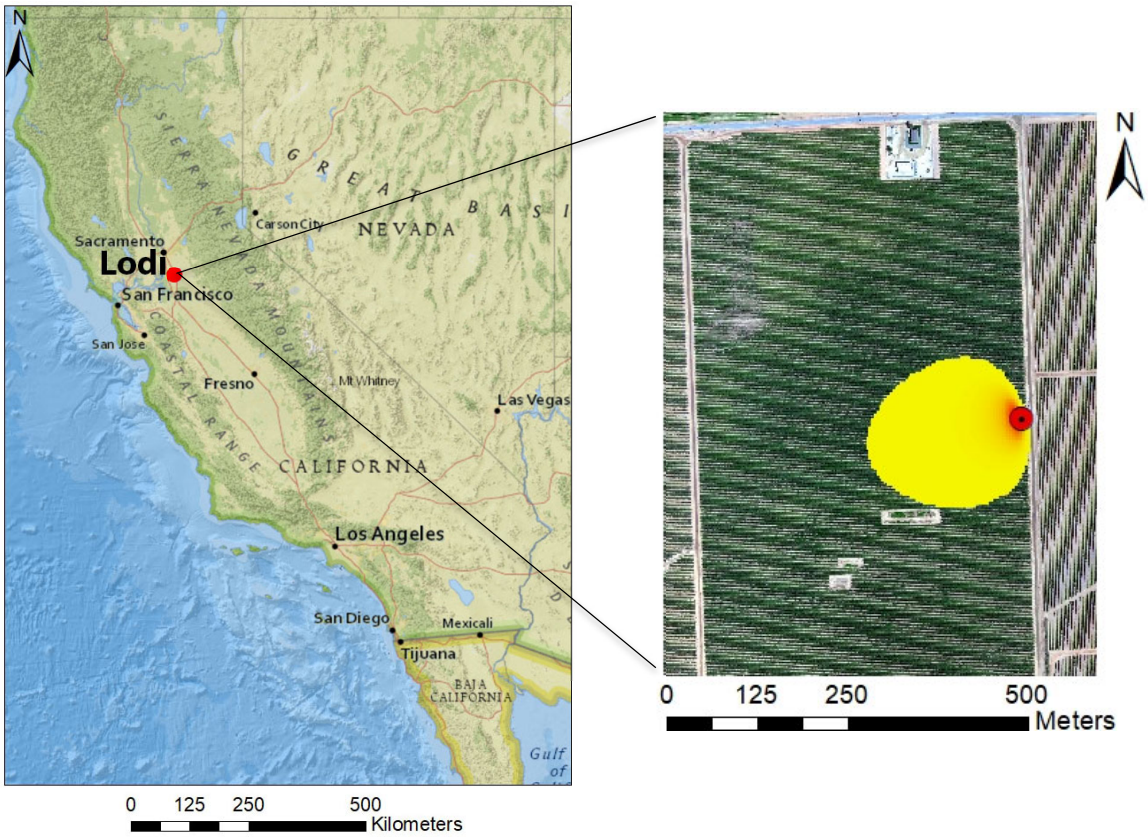

Figure 1. Layout of study area in Lodi, California, locations of the north EC tower, and an example of 90% of the EC footprint at Landsat time for August 09, 2014.

2.2 EC footprint model

Flux footprint models are used for interpretation of flux tower measurements to describe the position and size of surface source areas and the relative contribution of passive scalar sources to measured fluxes [11]. The flux footprint is defined as a mathematical function used to transfer between sources and sinks of passive scalars at the surface, Q_c, and the turbulent flux, F_c. Many parameters influence the estimate of the footprint, including receptor height, atmospheric stability, and surface roughness, all of which strongly affect the size of the footprint. The general mathematical expression used to describe the EC footprint analysis is shown in Equation (1)

$$F_c(0,0,z_m) = \int_{\Re} Q_c(x,y) f(x,y) dxdy \qquad (1)$$

where F_c is a flux density (per unit area), $Q_c(x,y)$ is the as source or sink at the surface. Because the footprint function is always estimated at a specific measurement height (receptor height), the vertical reference in f is neglected. From a single unit point source or sink,Q_u, Equation (1) can be simplified as follows

$$f(x,y) = \frac{F_c(0,0,z_m)}{Q_u(x,y)} \qquad (2)$$

In this study, the model used for footprint analysis was developed by Kljun et al. 2002 [23] using the three-dimensional Lagrangian stochastic footprint model LPDM-B. This model satisfies the well-mixed condition continuously for convective to stable stratifications and for measurement heights (receptors) within or above the surface layer. Assuming that crosswind turbulent dispersion can be treated independently from vertical or streamwise transport, the footprint function can be expressed in terms of a crosswind-integrated footprint, $f^{\overline{y}}$ and a cross-dispersion function, D_y

$$f(x,y) = \bar{f}^{y}(x)D_y \quad (3)$$

$$f(x,y) = \bar{f}^{y}\frac{1}{\sqrt{2\pi}\sigma_y}\exp\left(-\frac{y^2}{2{\sigma_y}^2}\right) \quad (4)$$

More details about the derivation of the footprint model and model parameters can be found at Kljun et al. 2015 [11]

2.3 TSEB2T model

For this research, the Two Source Energy Balance with a dual temperature (TSEB2T) model has been used. The TSEB model was originally developed by Norman et al. 1995 [24] to partition the radiative and turbulent fluxes between soil and canopy. In this case, net radiation (R_n) and latent heat flux (H) are partitioned between soil and canopy. TSEB has gone through several revisions to improve the representation of convective and radiative exchange between the soil and canopy system and the lower atmosphere. As illustrated in Figure (2), the TSEB2T model separates R_n, LE, and H between soil and vegetation, while G is calculated as a portion of R_{ns}. Equations (5-7) describe the mathematical expressions used for the TSEB2T model

$$R_n = LE + H + G, \quad (5)$$

$$R_{nc} = H_c + LE_c, \quad (6)$$

$$R_{ns} = H_s + LE_s + G, \quad (7)$$

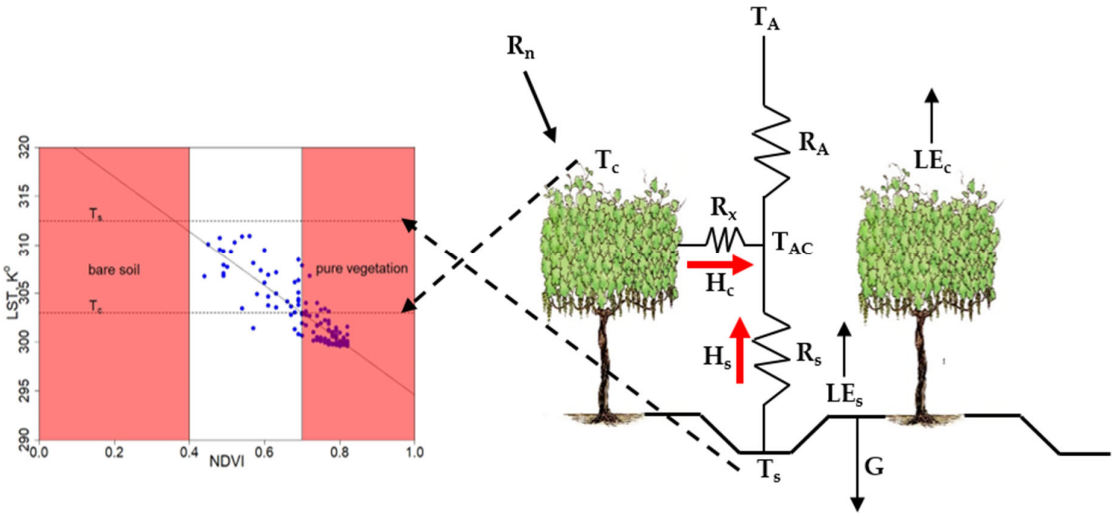

Figure 2. Schematic representation of the TSEB2T model

where R_n is the net radiation, H is the sensible heat flux, LE is the latent heat flux, and G is the soil heat flux. All flux units are in W/m^2. Subscripts of c and s represent the canopy and soil components, respectively. T_s and T_c represents the soil and canopy temperature, respectively and are derived from the LST using optical data with a high enough resolution. LE_c and LE_s are solved as residuals when (T_c and T_s) observations are available.

The main inputs of TSEB2T are T_c, T_s, f_c, LAI, w_c/h_c, and h_c, as well as ancillary micrometeorological data to parameterize the radiative and convective flux exchange between the soil/substrate and the canopy. A study conducted by Chirouze et al. 2014 [25] found the TSEB model to be better compared with other remote sensing ET models due to its lack of sensitivity to roughness.

The underpinning concept behind the TSEB2T model is the determination of T_s and T_c from composite LST imagery using the relationship between NDVI or any vegetation index (VIs) and LST, such as the LST-NDVI relationship [18]. T_s and T_c are then identified based on threshold values of NDVI for soil and canopy. Threshold $NDVI_c$ is calculated as the mean value of pixels identified as pure vegetation in a binary (soil-vegetation) classification of a

multispectral image. The NDVI threshold of pure soil for bare soil interrows is determined by constructing a relationship between NDVI and LAI curves when LAI in the interrows is nearly zero.

3. RESULTS

3.1 EC Footprint Estimation

Figure (3) represents the footprint analysis using the 2D flux model developed by Kljun et al. 2015 [11] and described in section 2.2 for a sUAS flight carried out on August 09, 2014. The fetch shape and orientation of the flux footprint / source area depend on the micro-meteorological conditions at the site measured by the EC towers. Those measurements involve turbulence fluxes, friction velocity, and wind speed, which affect atmospheric stability, and canopy and EC measurement height, which affect the effective sampling height and wind direction, subsequently affecting the orientation of the footprint. As illustrated in Figure (3), the different sizes of EC footprint fetch rely on the cutoff value used in the footprint analysis. A small EC fetch area relates to a low cutoff value, while a large contribution area / source area relates to a large cutoff value. The total statistical weight of the footprint is taken to equal unity by normalizing the values, although the actual area computed by the footprint model varies depending on the cutoff value.

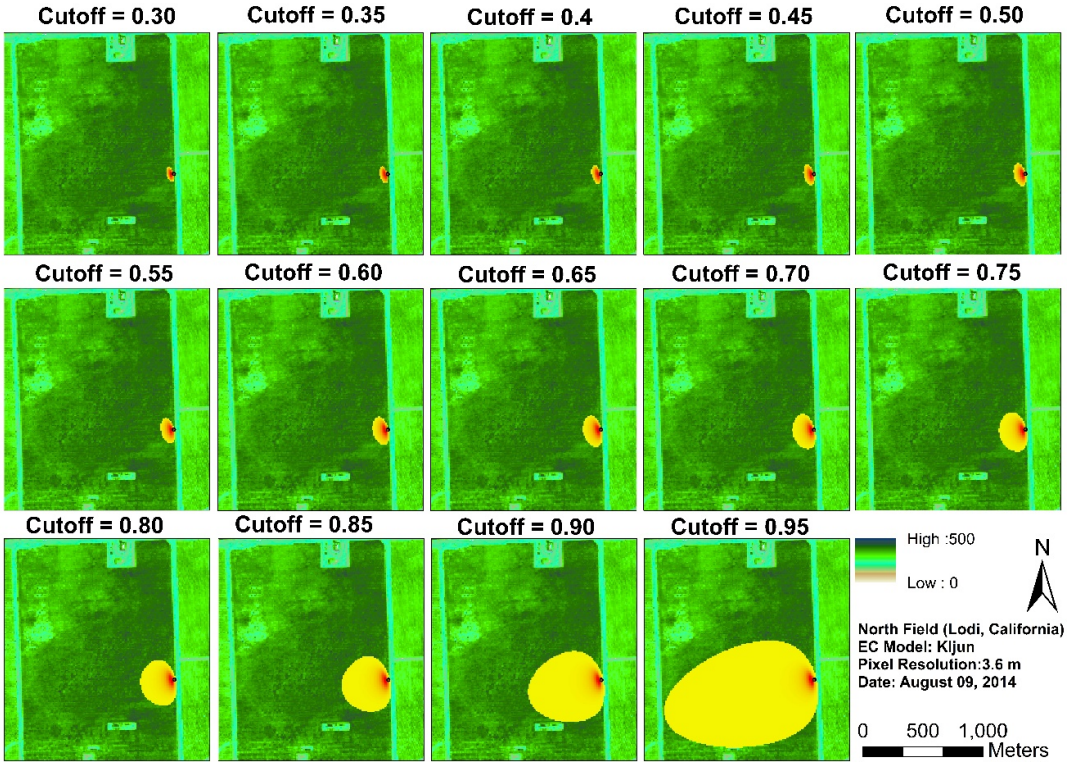

Figure 3. Multiple EC footprints at different cutoffs.

As shown in Figure (4), boxplots are used to demonstrate the variation of footprint weights within the source area across multiple cutoff values. The results indicate a decreasing trend in the weights as cutoff values increase. The highest weights with a large variance are observed at a 0.3 cutoff, while the lowest values with small variability are obtained when a 0.95 cutoff is used. At the 0.3 cutoff, a small number of pixels are involved inside the EC footprint, an area less than 700 m^2, which causes large deviations between the pixels located close to the EC towers and those at a large distance from the tower. In general, the highest weight in the footprint analysis is allocated to the closest pixels to the EC towers, which then degrade as the distance increases. Using a 0.95 cutoff, the results indicate a very small variation in the weights due to the large number of pixels included inside the source area / footprint, which give more

span / enough distance to the weights to decrease gradually, with the exception of some outliers (see Figure (4)) that represent the high-weighted pixels close to the EC tower.

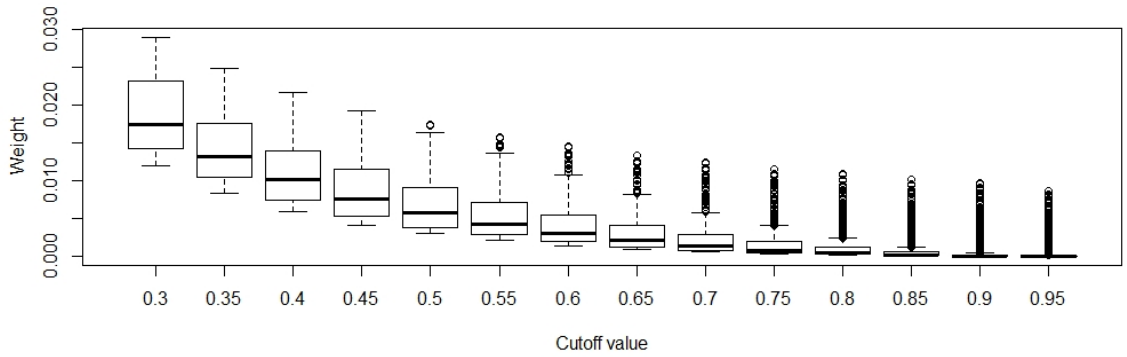

Figure 4. Boxplots for EC footprint weights at multiple cutoffs at 3.6-m resolution.

3.2 Impact of cutoff on LE statistics

To evaluate the effect of footprint cutoff on LE statistics inside the source area, multiple boxplots for LE values are presented (see Figure(5)), and other statistics including the mean, standard deviation, and coefficient of variation (CV) were calculated as shown in Table (1). As illustrated in Figure (5), although the results indicate an increasing variability in LE values as the cutoff value increases, a small shift in the median is observed across different cutoffs. The highest variation of LE was observed at a cutoff value of 0.95, ranging between 9 W/m^2 and 535 W/m^2, while, at 0.3 cutoff, the range becomes small, varying between 244 W/m^2 and 436 W/m^2. This happens due to the large number of pixels involved within the footprint domain at the 0.95 cutoff, whereas the 0.3 cutoff results in a small source area with a limited number of pixels, accounting for 54 units.

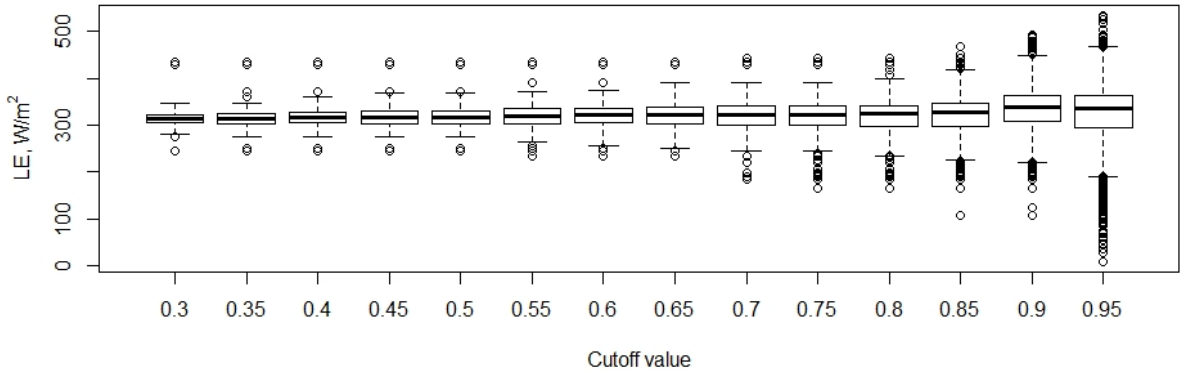

Figure 5. Boxplots of LE at multiple cutoffs at 3.6-m resolution.

As shown in Table 2, the mean (μ) shows little difference across different cutoff weights, with a slight increase in CV. In the range between the 0.3 and 0.65 cutoffs, the CV shows very close values that vary from 8% to 9%. The exception emerges at the 0.9 and 0.95 cutoffs, which show a significant difference in mean and CV. As demonstrated in Table 2, the mean at the 0.90 and 0.95 cutoffs yields values of 335 W/m^2 and 326 W/m^2, respectively, while the CV yielded values of 13% and 17%, respectively. This behavior aligns with the results presented in Figure (5) due to the large EC source area produced using high cutoff values, particularly at 0.95, which implies that more pixel units are included inside the footprint domain, causing high spatial variability.

Table 2. Statistics of sUAS TSEB2T LE inside the EC footprint/source area at different cutoffs.

Cutoff	Mean(W/m^2)	SD(W/m^2)	CV
0.3	317	29	9
0.35	316	29	9
0.4	317	27	9
0.45	318	27	8
0.5	318	27	8
0.55	319	27	9
0.6	321	26	8
0.65	321	28	9
0.7	320	31	10
0.75	319	34	11
0.8	318	35	11
0.85	320	39	12
0.9	335	44	13
0.95	326	54	17

Figure (6) shows the relationship between the cutoff and LE, calculated by multiplying the source area of the footprint model by the corresponding modeled LE map. The results indicate an increasing trend in LE with increasing cutoff value; however, the range of LE values is small, varying between 315 W/m^2 and 322 W/m^2. This implies that LE is only slightly influenced by the cutoff, particularly in the range between 0.6 and 0.85, which yield almost the same LE value of nearly 318 W/m^2. The best agreement between the modelled and measured LE is found at the 0.85 cutoff. Moreover, as illustrated in Figure (6), the general trend of the cutoff-LE relationship seems to behave like an exponential model within the cutoff range between 0.3 and 0.8, similar to a semivariogram plot, which is characterized by a linear increasing trend to a certain level that then flattens out.

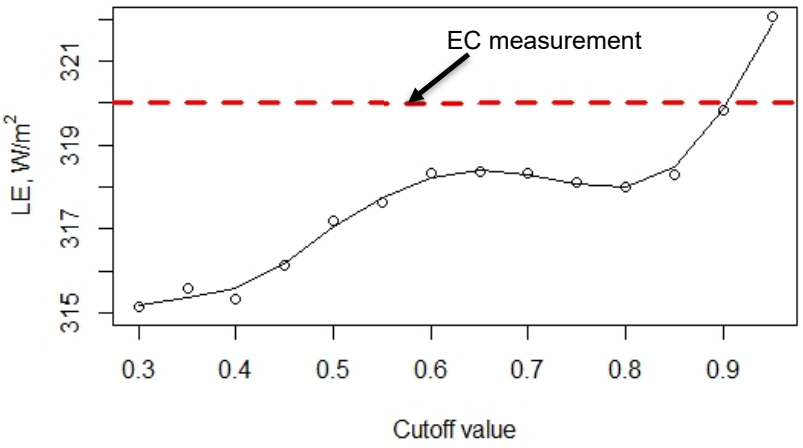

Figure 6. Relationship between the cutoff and the weighted LE.

4. CONCLUSIONS

The objective of this study was to evaluate the impact of EC weight cutoff on latent heat flux (LE) in vineyards at different cutoff values, specifically, 0.3, 0.35, 0.4, 0.45, 0.5, 0.55, 0.6, 0.65, 0.7, 0.75, 0.8, 0.85, 0.9, and 0.95, using the Kljun EC model along with a physically-based ET model known as TSEB2T with sUAS information. In this study, a grid size of 3.6 m was used for analysis, which represents the finest pixel resolution that includes both vine canopy and interrow conditions. Multiple statistical measures were used to assess the effect of cutoff on the LE values. Firstly, multiple boxplots were used to evaluate the weight of pixels inside the footprint domain, which indicate a decreasing trend in the weights with increasing cutoff values. High weights were observed at the 0.3 cutoff with large variation, while the 0.95 cutoff yielded very low values with little variation. Secondly, mean CV and bias were calculated to assess the LE statistics within the footprint domain at different cutoff values. The results indicate a high variation in LE values when large cutoff values were used, such as 0.9 and 0.95. This is because heterogeneity increases at larger footprints, thus providing a higher variability. The mean of LE from TSEB2T showed little difference across multiple cutoffs, with a slight increase in CV. The exception is at cutoff values of 0.9 and 0.95, which show a significant difference in mean and CV. Lastly, to assess the weighted LE values using different cutoff values, each source area estimated by the footprint model was multiplied by the corresponding modeled LE map produced by the TSEB2T model. The results indicate an increasing trend in LE with increasing cutoff value. However, the range of LE is very small, particularly when using cutoff values between 0.6 and 0.85. The best agreement between the modelled and measured LE is found at the 0.85 cutoff.

Funding: Funding was provided by E.&J. Gallo Winery. The Utah Water Research Laboratory contributed towards the acquisition and processing of the ground truth and sUAS imagery data collected during GRAPEX IOPs. We would like to acknowledge the financial support for this research from NASA Applied Sciences-Water Resources Program and the USDA Non Assistance Cooperative Agreement 58-8042-5-092 funding. USDA is an equal opportunity provider and employer.

Acknowledgments: We would like to thank the Aggieair Service Center team (Ian Gowing, Mark Winkelaar, and Shannon Syrstad) for their extraordinary support in this research, whose cooperation greatly improved the data collection and data processing, and the staff of the Viticulture, Chemistry and Enology Division of E.&J. Gallo Winery for their assistance in the collection and processing of field data during GRAPEX IOPs. This project would not have been possible without the cooperation of Mr. Ernie Dosio of Pacific Agri Lands Management, along with the Sierra Loma vineyard staff, for logistical support of GRAPEX field and research activities. The authors would like to thank Carri Richards for editing this paper.

Conflicts of Interest: The authors declare no conflict of interest.

5. REFERENCES

[1] "Eddy Covariance - an Overview | ScienceDirect Topics." n.d. Accessed March 1, 2020. https://www.sciencedirect.com/topics/earth-and-planetary-sciences/eddy-covariance.

[2] Blanken, P. D., T. A. Black, P. C. Yang, H. H. Neumann, Z. Nesic, R. Staebler, G. den Hartog, M. D. Novak, and X. Lee. 1997. "Energy Balance and Canopy Conductance of a Boreal Aspen Forest: Partitioning Overstory and Understory Components." Journal of Geophysical Research: Atmospheres. https://doi.org/10.1029/97jd00193.

[3] Constantin, J., A. Grelle, A. Ibrom, and K. Morgenstern. 1999. "Flux Partitioning between Understorey and Overstorey in a Boreal Spruce/pine Forest Determined by the Eddy Covariance Method." Agricultural and Forest Meteorology. https://doi.org/10.1016/s0168-1923(99)00129-x.

[4] Blanken, P. D., T. A. Black, H. H. Neumann, G. den Hartog, P. C. Yang, Z. Nesic, and X. Lee. 2001. "The Seasonal Water and Energy Exchange above and within a Boreal Aspen Forest." Journal of Hydrology. https://doi.org/10.1016/s0022-1694(01)00343-2.

[5] Wilson, Kell B., Paul J. Hanson, and Dennis D. Baldocchi. 2000. "Factors Controlling Evaporation and Energy Partitioning beneath a Deciduous Forest over an Annual Cycle." Agricultural and Forest Meteorology. https://doi.org/10.1016/s0168-1923(00)00124-6.

[6] Tuovinen, Juha-Pekka, Mika Aurela, Juha Hatakka, Aleksi Räsänen, Tarmo Virtanen, Juha Mikola, Viktor Ivakhov, Vladimir Kondratyev, and Tuomas Laurila. 2019. "Interpreting Eddy Covariance Data from Heterogeneous Siberian Tundra: Land-Cover-Specific Methane Fluxes and Spatial Representativeness." Biogeosciences. https://doi.org/10.5194/bg-16-255-2019.

[7] Virkkala, Anna-Maria, Tarmo Virtanen, Aleksi Lehtonen, Janne Rinne, and Miska Luoto. 2018. "The Current State of CO2 Flux Chamber Studies in the Arctic Tundra." Progress in Physical Geography: Earth and Environment. https://doi.org/10.1177/0309133317745784.

[8] Schmid, Hans Peter. 2002. "Footprint Modeling for Vegetation Atmosphere Exchange Studies: A Review and Perspective." Agricultural and Forest Meteorology. https://doi.org/10.1016/s0168-1923(02)00107-7.

[9] Mauder, Matthias, Matthias Cuntz, Clemens Drüe, Alexander Graf, Corinna Rebmann, Hans Peter Schmid, Marius Schmidt, and Rainer Steinbrecher. 2013. "A Strategy for Quality and Uncertainty Assessment of Long-Term Eddy-Covariance Measurements." Agricultural and Forest Meteorology. https://doi.org/10.1016/j.agrformet.2012.09.006.

[10] Göckede, M., T. Foken, M. Aubinet, M. Aurela, J. Banza, C. Bernhofer, J. M. Bonnefond, et al. 2008. "Quality Control of CarboEurope Flux Data – Part 1: Coupling Footprint Analyses with Flux Data Quality Assessment to Evaluate Sites in Forest Ecosystems." Biogeosciences. https://doi.org/10.5194/bg-5-433-2008.

[11] Kljun, N., P. Calanca, M. W. Rotach, and H. P. Schmid. 2015. "A Simple Two-Dimensional Parameterisation for Flux Footprint Prediction (FFP)." Geoscientific Model Development 8 (11): 3695–3713.

[12] Anderson, Cody A., and Enrique R. Vivoni. 2016. "Impact of Land Surface States within the Flux Footprint on Daytime Land-Atmosphere Coupling in Two Semiarid Ecosystems of the Southwestern U.S." Water Resources Research. https://doi.org/10.1002/2015wr018016.

[13] McKee, Mac, Ayman Nassar, Alfonso Torres-Rua, Mahyar Aboutalebi, and William Kustas. 2018. "Implications of Sensor Inconsistencies and Remote Sensing Error in the Use of Small Unmanned Aerial Systems for Generation of Information Products for Agricultural Management." Proceedings of SPIE The International Society for Optical Engineering 10664 (July). https://doi.org/10.1117/12.2305826.

[14] Nassar, Ayman; Nieto, Hector; Aboutalebi, Mahyar; Torres-Rua, Alfonso; McKee, Mac; Kustas, William; Prueger, John; McKee, Lynn; Alfieri, Joseph; Hipps, Lawrence; et al. Pixel Resolution Sensitivity Analysis for the Estimation of Evapotranspiration Using the Two Source Energy Balance Model and sUAS Imagery under Agricultural Complex Canopy Environments; American Geophysical Union (AGU): Washington, DC, USA, 2018

[15] Nassar, Ayman; Torres-Rua, Alfonso; Alfieri, Joseph; Hipps, Lawrence; Prueger, John; Nieto, Hector; Alsina, Maria; McKee, Lynn; White, William; Kustas, William; McKee, Mac; Coopmans, Calvin; Sanchez, Luis; Dokoozlian, N. Assessment of High-Resolution Daily Evapotranspiration Models Using Instantaneous sUAS ET in Grapevine Vineyards; American Geophysical Union (AGU): California, USA, 2019

[16] Nassar, Ayman; Torres-Rua, Alfonso; McKee, Mac; Kustas, William; Coopmans, Calvin; Nieto, Hector; Hipps, Lawerence. Assessment of UAV Flight Times for Estimation of Daily High Resolution Evapotranspiration in Complex Agricultural Canopy Environments. UCOWR/NIWR Annual Water Resources Conference: Utah, USA, 2019

[17] Nassar, Ayman, Alfonso F. Torres-Rua, Joseph G. Alfieri, Lawrence E. Hipps, John H. Prueger, Hector Nieto, Maria Mar Alsina, et al. 2020. "To What Extend Does the Eddy Covariance Footprint Cutoff Influence the Estimation of Surface Energy Fluxes Using Two Source Energy Balance Model and High-Resolution Imagery in Commercial Vineyards? (Conference Presentation)." Autonomous Air and Ground Sensing Systems for Agricultural Optimization and Phenotyping V. https://doi.org/10.1117/12.2558777.

[18] Nassar, Ayman, Alfonso Torres-Rua, William Kustas, Hector Nieto, Mac McKee, Lawrence Hipps, David Stevens, et al. 2020. "Influence of Model Grid Size on the Estimation of Surface Fluxes Using the Two Source Energy Balance Model and sUAS Imagery in Vineyards." Remote Sensing. https://doi.org/10.3390/rs12030342.

[19] Nassar, Ayman, Alfonso F. Torres-Rua, Hector Nieto, Joseph G. Alfieri, Lawrence E. Hipps, John H. Prueger, Maria M. Alsina, et al. 2020. "Implications of Soil and Canopy Temperature Uncertainty in the Estimation of Surface Energy Fluxes Using TSEB2T and High-Resolution Imagery in Commercial Vineyards (Conference Presentation)." Autonomous Air and Ground Sensing Systems for Agricultural Optimization and Phenotyping V. https://doi.org/10.1117/12.2558715.

[20] Torres-Rua, Alfonso F., Mahyar Aboutalebi, Timothy Wright, Ayman Nassar, Pierre Guillevic, Lawrence Hipps, Feng Gao, et al. 2019. "Estimation of Surface Thermal Emissivity in a Vineyard for UAV Microbolometer Thermal Cameras Using NASA HyTES Hyperspectral Thermal, and Landsat and AggieAir Optical Data." Autonomous Air and Ground Sensing Systems for Agricultural Optimization and Phenotyping IV. https://doi.org/10.1117/12.2518958.

[21] McKee, Mac, Alfonso F. Torres-Rua, Mahyar Aboutalebi, Ayman Nassar, Calvin Coopmans, William P. Kustas, Feng Gao, Nicholas Dokoozlian, Luis Sanchez, and Maria M. Alsina. 2019. "Challenges That beyond-Visual-Line-of-Sight Technology Will Create for UAS-Based Remote Sensing in Agriculture (Conference Presentation)." Autonomous Air and Ground Sensing Systems for Agricultural Optimization and Phenotyping IV. https://doi.org/10.1117/12.2520248.

[22] Torres-Rua, Alfonso. 2017. "Vicarious Calibration of sUAS Microbolometer Temperature Imagery for Estimation of Radiometric Land Surface Temperature." Sensors 17 (7). https://doi.org/10.3390/s17071499.

[23] Kljun, N., M. W. Rotach, and H. P. Schmid. 2002. "A Three-Dimensional Backward Lagrangian Footprint Model For A Wide Range Of Boundary-Layer Stratifications." Boundary-Layer Meteorology. https://doi.org/10.1023/a:1014556300021

[24] Norman, J. M., W. P. Kustas, and K. S. Humes. 1995. "Source Approach for Estimating Soil and Vegetation Energy Fluxes in Observations of Directional Radiometric Surface Temperature." Agricultural and Forest Meteorology. https://doi.org/10.1016/0168-1923(95)02265-y.

[25] Chirouze, J., G. Boulet, L. Jarlan, R. Fieuzal, J. C. Rodriguez, J. Ezzahar, S. Er-Raki, et al. 2014. "Intercomparison of Four Remote-Sensing-Based Energy Balance Methods to Retrieve Surface Evapotranspiration and Water Stress of Irrigated Fields in Semi-Arid Climate." Hydrology and Earth System Sciences. https://doi.org/10.5194/hess-18-1165-2014.